Predicting the structure of screw dislocations in nanoporous materials

ANDREW M. WALKER[1,2]*, BEN SLATER[1]*, JULIAN D. GALE[3] AND KATE WRIGHT[1,2,4]

[1]Davy Faraday Research Laboratory, The Royal Institution of Great Britain, 21 Albemarle Street, London, W1S 4BS, UK
[2]Department of Earth Sciences, University College London, Gower Street, London, WC1E 6BT, UK
[3]Nanochemistry Research Institute, Department of Applied Chemistry, Curtin University of Technology, PO Box U1987, Perth, Western Australia
[4]Department of Chemistry, Christopher Ingold Laboratories, University College London, 20 Gordon Street, London, WC1H 0AJ, UK
*e-mail: andreww@ri.ac.uk; ben@ri.ac.uk

Published online: 7 September 2004; doi:10.1038/nmat1213

Extended microscale crystal defects, including dislocations and stacking faults, can radically alter the properties of technologically important materials. Determining the atomic structure and the influence of defects on properties remains a major experimental and computational challenge. Using a newly developed simulation technique, the structure of the 1/2**a** <100> screw dislocation in nanoporous zeolite A has been modelled. The predicted channel structure has a spiral form that resembles a nanoscale corkscrew. Our findings suggest that the dislocation will enhance the transport of molecules from the surface to the interior of the crystal while retarding transport parallel to the surface. Crucially, the dislocation creates an activated, locally chiral environment that may have enantioselective applications. These predictions highlight the influence that microscale defects have on the properties of structurally complex materials, in addition to their pivotal role in crystal growth.

In the quest to optimize the efficiency of materials, attention is increasingly focused from the nanoscale to understanding how microscale defects, such as stacking faults and dislocations, affect the properties of materials. In some instances, these defects are ruinous; for example, in the manufacture of silicon computer chips, suppression of dislocations in silicon wafers is absolutely crucial, because the conductivity changes when dislocations are present. Zeolitic materials are used extensively within the petrochemical and fine chemical industries, where the integrity of the crystal's structure is often vital to the catalytic efficiency of that material[1]. This porous class of materials contains cages and channels of molecular dimensions that permit selective diffusion within the host material, thus leading to their widespread use as molecular sieves and catalysts. The channel diameter ranges from ~4–15 Å in 'microporous' materials to greatly in excess of 30 Å in 'mesoporous' materials, offering the possibility of extensive tunability for specific applications.

When zeolites are chosen for selectivity towards a particular molecular dimension it is often presumed that they contain regular pores with uniform dimensions, except when chemical substitution within the framework topology has taken place. However, the very channel structure itself may be distorted and displaced by extended defects leading to significant changes in transport behaviour. It is of particular interest to interpret how transport and reactivity within nanoporous materials is affected by the presence of defects whose length scale varies from a few to several hundred ångströms. Rather exotic defects—such as co-incidence boundaries in zeolite L—have been observed, and these are thought to dramatically reduce intracrystal molecular transport rates[2]. Framework materials also commonly exhibit linear chain defects, such as those recently described in mordenite[3]. Other extended defects, including stacking faults and growth spirals, have previously been studied within the crystal bulk and at the surface. However, although dislocations have been widely observed and modelled in materials such as metals[4–7], semiconductors[8–12] and some simple ceramics[13–20], there have been few attempts to characterize these clusters in many other more complex materials. Surprisingly, almost nothing is known about what effect

©2004 Nature Publishing Group

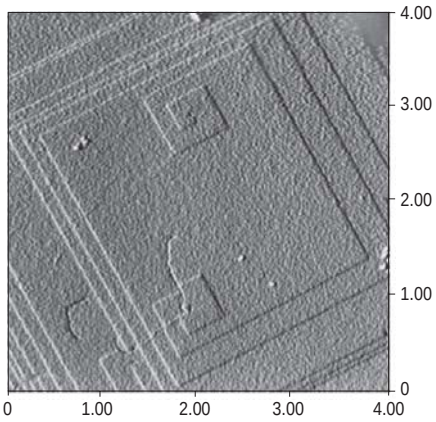

Figure 1 **AFM image of growth spirals on the {100} surface of synthetic zeolite A taken from ref. 21.** The spirals are caused by growth at steps that are due to the emergence of screw dislocations at the surface. The steps are reported to be 1.2 nm high and the field of view is 4 μm across. Reprinted from ref. 21 Copyright (2002), with permission from Elsevier.

dislocations have on the properties of zeolites. In this article, we address this point by examining the atomic structure of a screw dislocation in zeolite A. To the best of our knowledge, this is the first reported model of a dislocation in a structurally complex material of any kind. We believe that the results have important implications for molecular transport and reactivity in zeolites, and for porous materials in general.

Our motivation to study zeolite A (LTA) was inspired by the exceptional recent high-resolution atomic force microscopy (AFM) observation of growth spirals on its {100} surface[21]. These growth spirals (Fig. 1), clearly show the presence of screw dislocations emerging from the interior of the crystal, thus providing steps on the surface that can act as very favourable sites for growth. Unlike the case of an 'ideal' crystal surface, where steps are extinguished when a full crystal layer is formed, the step is continually regenerated as layer after layer of material is added to the surface. This process avoids the rate-limiting step in crystal growth, which is normally considered to be the addition of a growth unit to the perfect surface[22].

Although it is clear that dislocations play a vital role in controlling the growth of materials such as LTA[21], heulandite[23] and presumably many other zeolitic materials, we do not know what effect they have on structure and reactivity. Although the technique of AFM can reveal the presence of dislocations at the surface it cannot yield atomic-scale resolution of the structure of the dislocation core, and thus the properties of this defect cannot be readily inferred or deduced. However, using simulation methods we explicitly have atomic resolution, which enables us to analyse how the dislocation core structure affects zeolite transport and reactivity.

Zeolite A has the structural formula $[Na_{12}(H_2O)_{27}]_8[Al_{12}Si_{12}O_{48}]_8$ and was one of the first zeolites to be commercially exploited, in particular as an ion-exchanger within clothing detergents. It continues to be manufactured on a massive scale worldwide and has inspired widespread experimental[24,25] and computational[24–26] investigation. The structure consists of a three-dimensional interconnecting network of channels, which permits transport through the crystal, and two cage structures defined by the aluminosilicate framework; the alpha cage shown in Fig. 2a and beta (or sodalite) cage shown in Fig. 2b. Diffusion through the structure occurs through the channel system, where the narrowest points within the accessible void space are at each of the largest faces of the alpha cage, at an eight-membered ring with a diameter 6.8 Å (Fig. 3a). The narrowest point provides the largest barrier to transport and hence determines the diffusion rate for the non-defective structure.

Details of our simulation model are described later, but in essence, an atomistic model of the dislocation core is embedded within an elastic description of the infinite crystal at long range. The simulation 'cell' is in fact a cylinder, which is periodic in one dimension only, parallel to the dislocation core. The cell is first generated from the energy minimized bulk structure of LTA, and then the required elastic deformation to introduce the dislocation is applied. When the radius of the simulation cell is sufficiently large, the structure of the cell perimeter generated by the linear elastic displacement will be correct and only the structure close to the core requires relaxation. This is achieved by performing an atomistic structural optimization using a forcefield approach. To minimize boundary effects the simulation cell is embedded within a sheath of fixed ions, which represent the infinite crystal. Here we treat the LTA structure as being purely siliceous for simplicity and this captures the dominant effect—namely the effect of the change in topology. The secondary effect on extra-framework cations is reserved for future work.

In dense materials, the dislocation core greatly distorts the structure, but one recognises that in very porous materials the deformation origin can be sited in empty space, thus reducing the energetic cost of introducing the defect. In LTA, the most obvious location for the dislocation is at the centre of an alpha cage, where the vector will naturally run along the centre of the eight-ring channels (Fig. 3a) responsible for diffusion. Alternative dislocation origins have been examined, but all of these are found to be unstable with respect to the origin described here. After the dislocation is introduced, the eight-membered rings at the interface between alpha cages form a helix along the dislocation line, shown in Fig. 3c. We note that the height of the dislocation reported by Dumrul *et al.*[21] is 1.2 nm, which corresponds exactly with 1/2a, equal to the length of the Burgers vector. Regular step or terrace heights on apparently non-dislocated samples have also been measured to be 1.2 nm by Agger and co-workers[24]. The fact that the measured step height and our predicted Burgers vector magnitude are equal provides strong evidence that we have correctly modelled the dislocated core of the zeolite. Another significance of this distance is that it corresponds to the height of the alpha cage. From consideration of previous surface structure determinations[27], we anticipate that when the screw dislocation terminates at the surface, a complete alpha cage will be expressed.

After relaxation of the structure, we find that atoms closest to the core are displaced away from the channel centre by up to ~0.15 Å. The displacements of atoms relative to their original position follow an approximately oscillatory pattern, where an alternate expansion and contraction of the radial coordination shells is observed. The silicon atoms are more strongly perturbed than the oxygen atoms; and the magnitude of the displacements attenuate quite slowly, but beyond 20–30 Å the channels will correspond almost exactly to those of the non-defective material. Along the dislocation line, the displacements are more extensive with a maximum magnitude of ~0.4 Å and again, the silicon atoms relax more than the oxygen atoms. The net effect of these displacements is outlined in the Supplementary Information (Fig. S1 and Table S1), but briefly, the length of the central helical structure is longer than the original channel. The uniform elastic approximation used to generate the initial coordinates for the dislocation leads primarily to extension of the Si–O bond lengths. On relaxation, the Si–O–Si bond angles increase in order to reduce the bond length elongation.

In Fig. 4, we have highlighted the central core of both the non-defective and dislocated material. Here, we display the surface of the inaccessible volume of the material, which is impermeable to small molecules. In Fig. 4a, which corresponds to looking down on the {100} surface, one can clearly see the perfectly regular channel systems. Similarly, in Fig. 4b, which corresponds to a cross-section through the

©2004 Nature Publishing Group

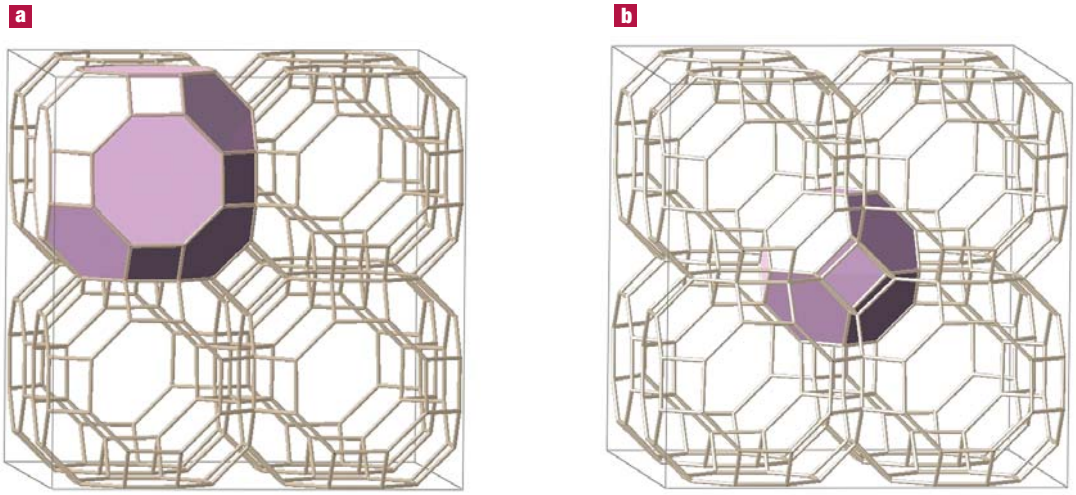

Figure 2 **Topology of zeolite A based on the silica framework. a**, The alpha cage. **b**, The beta or sodalite cage. The alpha cages, joined by eight-rings, form the three perpendicular sets of channels, the sodalite cages joined by double four-rings are relatively impermeable.

surface, regular, circular channels are seen. Turning to the dislocated system, in Fig. 4d where the core atoms that comprise the eight-ring helix are highlighted in pink, the central channel appears to be unperturbed, and clearly the channel extends into the host without obstructions. However, if we examine the 'surface' cross section in Fig. 4e, we see that the channel system has apparently become blocked by the presence of the central dislocation. The neighbouring channels, although deformed from a circular to oval cross-section, are not obstructed. A planar cross-section of the channel is shown in atomic detail in Fig. 3b and further data is given in the Supplementary Information. The important feature of this elliptical distortion is that the channel has different minimum and maximum dimensions from the original channel. The minimum distance is reduced from 6.78 Å to 5.95 Å, while the maximum distance is increased to 7.80 Å. The implications that these structural deformations have for molecular transport are discussed later.

To spatially image the cage systems that surround the dislocation, we plot the surface that bounds the accessible volume, to show where small molecules and ions with their hydration shell can diffuse through. In Fig. 4f, the core we have shown earlier is clipped to reveal the channel and cage system around the dislocation. Intriguingly, the effect of the dislocation is almost completely to equalize the diameter of the channel

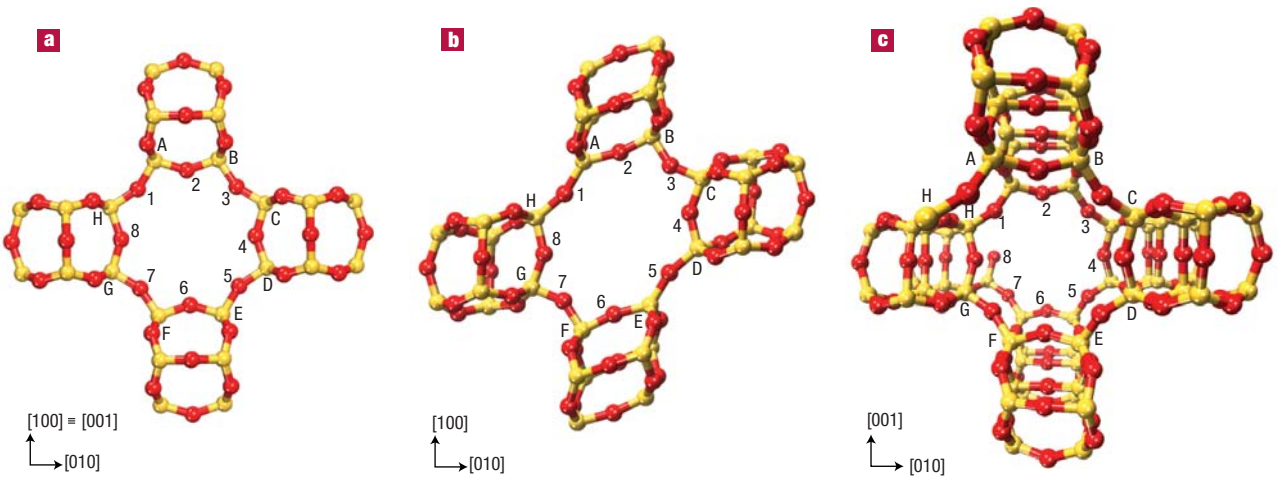

Figure 3 **Views of three eight-ring structures in zeolite A. a**, An eight-ring in perfect zeolite A viewed along <100>, note the presence of a fourfold rotation axis in the centre of the ring. **b**, Eight-ring opening onto the central channel of the dislocated zeolite, the fourfold axis is lost (and becomes a twofold axis) and the opening becomes significantly deformed. Assuming Burgers vector lies along [100] this is a view along [010] or [001]. **c**, A perspective view down the central channel (along [100]) containing the dislocation core, the eight-ring structure is cut and fuses with adjacent eight-rings to form a continuous helix but the symmetry is maintained. Numbers and letters refer to oxygen and silicon atoms listed in Table S1 of the Supplementary Information.

©2004 Nature Publishing Group

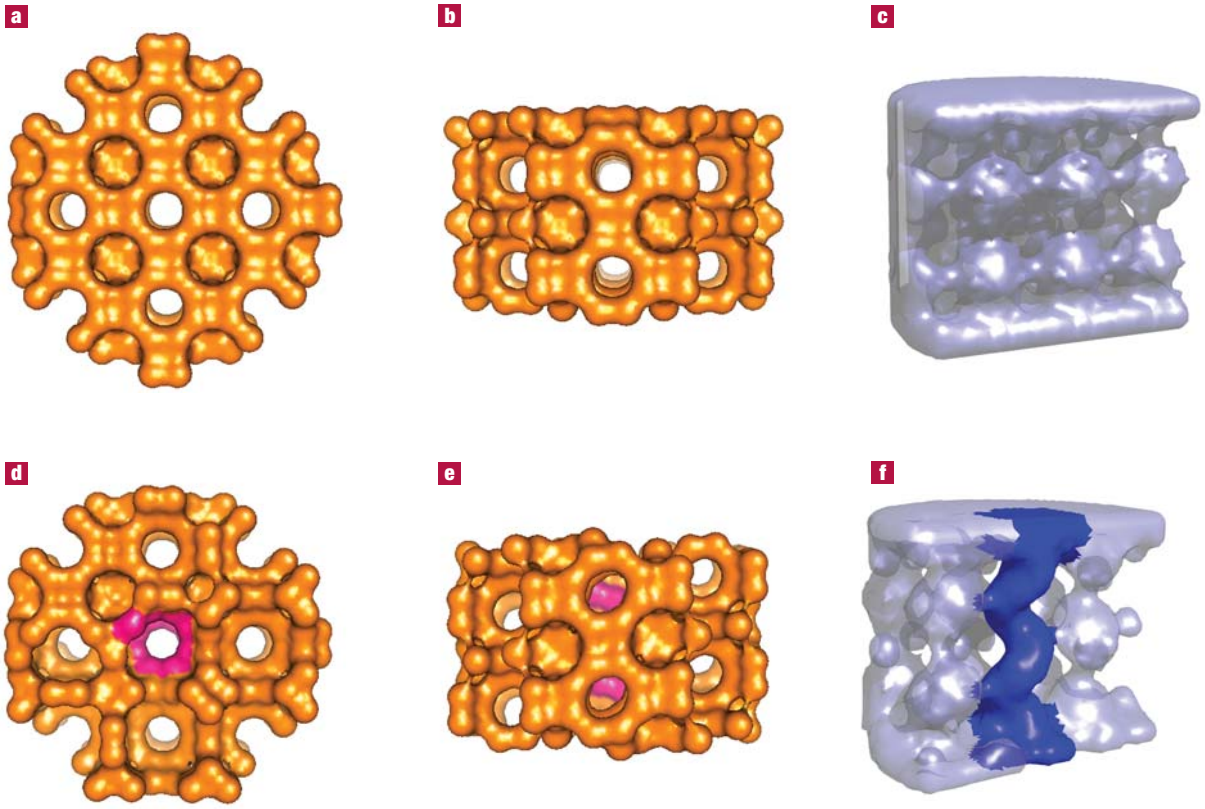

Figure 4 **Channel systems in perfect and dislocated zeolite A. a**–**c**, The bulk system. **d**–**f**, The dislocated system. Parts **a**, **b**, **d** and **e** are the surface of the inaccessible volume viewed down (**a** and **d**) and across (**b** and **e**) the dislocation line. Parts **c** and **f** show the surface accessible volume, with the central helix highlighted in blue.

to give a helical tube with a prescribed handedness as seen in Fig. 1. The effect can be loosely equated to the magic trick where a knotted length of rope is gently pulled and the knots disappear. The neighbouring channels are distorted, but are much more closely related to the perfect lattice system than the dislocation core, which forms a near perfectly regular channel.

It is clear that the effect of the dislocation on the channel system is dramatic, and we can expect that molecular transport will be considerably modified. Computer simulation of molecular transport in zeolites is a well-studied field, where very detailed and comprehensive investigations into jump dynamics at pinch points or bottlenecks within zeolites have been reported[28,29]. It is beyond the scope and aim of this paper to analyse quantitatively how the critical barrier heights for transport are affected, however, qualitative predictions can be made on simple geometric grounds. Because the diameter of the core channel is larger, access from the surface to the core interior will be easier than in channels in the non-defective material, thereby permitting larger molecules to access the crystal interior. Diffusion parallel to the surface is, however, regulated by the distorted eight rings and thus transport of molecules with a kinetic diameter exceeding that of the eight-membered ring perpendicular to the dislocation core will be severely retarded. In LTA, because of the size of the dislocation vector, the channel systems become misaligned by 1/2a, as is depicted in Fig. 4e. The guest molecule diffuses to the core region and then has to follow a branch to another channel to continue its traversal across the system. In effect, the dislocation scatters diffusing species by rotating their direction of motion. It would seem likely that even at moderate partial pressures, molecules would have a relatively high residence time in the vicinity of dislocation core, and this could lead to a substantial reduction of the gross 'flux density' of gas through the material. The overall reduction of the flux clearly depends on the dislocation density. Although the density of the dislocations is likely to be small, it has already been demonstrated that the structure is perturbed out to a range of 20–30 Å, and so the total volume influenced by the dislocation may be far from negligible.

On examining the shape of the dislocation core, the helical structure implies a local chirality and so we expect that different enantiomers will diffuse through the core at inequivalent rates. The overall material may of course be racemic if an equal number of dislocations of opposite handedness exist. However, the enantiomers will become spatially partitioned within separate dislocations in the material, a phenomenon that could be exploited in enantioselection technologies.

Finally, we turn to the question of how the reactive properties of the core may be different to those of the internal surface of the perfect crystal. Because the eight-membered ring is distended along *a*, it follows that all the Si–O (and Al–O in the real system) bond lengths are extended. The quantitative extent to which this occurs in the present model is highlighted in the Supplementary Information, though we emphasize that the importance is in the trend, rather than the absolute magnitude of the changes in bond length. Analysis of the correlation between Si–O bond length and the 'reactivity' is not simple; Si–O–Si bond lengths and angles can adopt a myriad of values with a remarkably minor energetic penalty[30], as is evident from the many purely siliceous zeolitic structures, with extremely varied pore systems and reactive properties. However, given that the Si–O bond length is extended, it follows that the bond is weakened, and it will therefore be more vulnerable to attack by, for example, hydrolysis and therefore

©2004 Nature Publishing Group

dissolution or exchange of framework aluminium. It is also likely, therefore, that the core interior will be more acidic than an ideal channel, which will permit different chemistry to occur.

Our calculations yield an atomic structure for a dislocation core in zeolite A that is consistent with the current experimental data, and will provide a strong basis for the interpretation of future work. The considerable distortion of the local channel structure will bestow very different properties on the region surrounding the dislocation, especially with respect to molecular diffusivities. This may be especially important for aligned composite zeolite membranes, such as that described by Lai *et al.*[1]. Although our study pertains to LTA, our technique is general and can be applied to many other complex materials where the behaviour of the dislocation core is crucial to understanding a range of properties (A.M.W., J.D.G., B.S. and K.W., manuscript in preparation). Examples include water ice (where dislocations contribute to the rheological behaviour of glaciers, and of the Jovian moons[31] and the morphology of snow crystals[32]) and olivine, which deforms through the movement of dislocations[33] allowing terrestrial plate tectonics. We also contend that screw dislocations in many other zeolitic materials will be imbued with distinct reactive and transport properties that may well influence the behaviour of these technologically important materials.

METHODS

Our model of the screw dislocation in zeolite A is based on a combined atomistic–elastic model that will be described in detail elsewhere (A.M.W., J.D.G., B.S. and K.W., manuscript in preparation). Linear elastic theory is sufficient to describe the structure of a dislocated crystal away from the dislocation core. However, close to the core strains are large and nonlinear terms make a significant contribution. Additionally, reconstruction of the atomic structure of the core itself may be important and such reconstructions cannot be described by a continuum theory. The atoms in and around the core are therefore described using a parameterized potential function based on the Born model of solids, incorporating ionic polarizability. This atomic model is embedded in an elastic continuum, which represents the infinite crystal. In common with previous studies of simple metal oxides the dislocation line is assumed to be straight and uniform, a situation enforced by the application of a periodic boundary condition in one dimension.

To simplify the description of zeolite A, we have used a purely siliceous model, which crucially allows us to comment on the deformation of the structure near to the dislocation and to interpret how the perturbation of the lattice will affect transport properties of the system. The functional form of our forcefield is chosen so as to closely resemble the model of Sanders *et al.*[34], which has been used successfully for two decades now in the simulation of silicate phases[30], except that in this model the potential decays smoothly to zero at inter-atomic separations of 8 Å. The real-space Wolf summation[35] is used for the Coulomb part of the potential model, thus allowing a spatial decomposition scheme to be used for the total energy summations. Using this approach, the calculations scale linearly with system size, making it feasible to study the hundreds of thousands of atoms required for well-converged dislocation simulations. We use the latest revision of the GULP code to perform the calculations[36]. Further details and parameters of the potential model are available in the Supplementary Information. However, the key point to note is that the model is designed to reproduce not only the structural parameters of α-quartz, but also the curvature-related physical properties. This implies that the model should be at least qualitatively reliable for the study of elastic distortions of silica phases.

In the readily synthesised form of zeolite A, with a Si/Al ratio of 1:1, it has been shown that aluminium and silicon strictly order with alternate Si–O–Al bonding in agreement with Löwenstein's rule[37]. It follows that only every other beta cage is equivalent by translation and the structure takes on a face-centred-cubic (f.c.c.) structure (space group $Fm\bar{3}c$) with cell parameter 24.61 Å, thereby avoiding Al–O–Al linkages, which have been demonstrated to be energetically unfeasible on this length scale[38]. According to standard dislocation theory[39] the Burgers vector of any dislocation should be an integer multiple of one of the primitive lattice vectors where the elastic energy of the dislocation is proportional to the square of the length of the Burgers vector. Applying this to f.c.c. LTA suggests that the lowest-energy Burgers vector will lie along <110> with length $\sqrt{(1/2a)}$ (where a is the lattice vector parallel to the *a* axis of magnitude ~24 Å) followed by a Burgers vector along <100> with a length equal to a (Fig. S2a in the Supplementary Information). However, in an ordered framework material there is a possibility that the Burgers vector may be commensurate with the topological symmetry, rather than that of the crystal unit cell. In this instance, which is rather analogous to 'superlattices' of ordered solid solutions such as beta brass[22], the shortest, and hence lowest energy, Burgers vector would be the 1/2a <100> screw dislocation, which has length ~12 Å, as shown in Fig. S2b. As the introduction of this dislocation has the lowest energetic penalty (because it has the shortest Burgers vector) this is the only model we have fully relaxed. However, single point energy calculations of the 1a <100> screw dislocation confirm that its energy is very much higher than the 1/2a dislocation model reported here.

We set up the simulation by first generating a large cylindrical cell of height 24 Å and radius 115 Å. This cell contains ~68,000 ion centres. We have checked for finite size effects using a cell of approximately twice this radius (~250,000 centres, 215 Å radius) and found no evidence that the relaxation was constrained in the smaller cell. Charge neutrality is achieved by building the cell from neutral SiO_4 units (assigning each oxygen a charge of –1). Oxygen ions within the cell that belong to two units, then have a formal charge of –2, as they 'belong' to two SiO_4 units, whereas those at the edge of the simulation cell, which only co-ordinate one silicon ion, have a charge of –1. The cell is terminated only with oxygen ions, and all silicon ions are fully co-ordinated. Enforcing this condition minimizes the dipole moment across the cell. Cancellation of the residual dipole (~0.2 e Å) was found to alter the total energy of the simulation cell by less than 1×10^{-5} eV, which is insignificant in comparison with thermal energy. The screw dislocation is then introduced assuming linear elasticity with the origin of the elastic displacement field located along the centre on one of the eight-ring channels (in this case the anisotropic elastic solution to the displacement field reduces to the more familiar isotropic form[40]) for all the simulation atoms. Finally, the total energy of the simulation cell is minimized by varying the positions of atoms within 100 Å (or 200 Å, for the larger cell) of the centre of the cell using a conjugate gradients algorithm.

For computational simplicity we do not allow the elastic region of the model to respond to forces generated in the atomistic region; we use fixed boundary conditions[15,19] rather than flexible boundary conditions[4,3,41–43]. A consequence of this is that forces and displacements across the atomic–elastic boundary are discontinuous. However, because the cell size is very large this is not likely to affect the structure of the core itself, though the discontinuity can be seen in the Supplementary Information, Fig. S1. The extremely flexible Si–O–Si bonds rapidly screen perturbations within the framework; hence we believe that the fixed boundary conditions are entirely appropriate for this material.

Received 19 February 2004; accepted 28 July 2004; published 7 September 2004.

References

1. Lai, Z. P. *et al.* Microstructural optimization of a zeolite membrane for organic vapor separation. *Science* 300, 456–460 (2003).
2. Terasaki, O., Thomas, J. M. & Ramdas, S. A new type of stacking-fault in zeolites - presence of a coincidence boundary (square-root 13. square-root 13 R32.2-degrees superstructure) perpendicular to the tunnel direction in zeolite-L. *J. Chem. Soc. Chem. Commun.* 216–217 (1984).
3. Campbell, B. J. & Cheetham, A. K. Linear framework defects in zeolite mordenite. *J. Phys. Chem.* 106, 57–62 (2002).
4. Sinclair, J. E. Improved atomistic model of a bcc dislocation core. *J. Appl. Phys.* 42, 5321–5329 (1971).
5. Gehlen, P. C., Hirth, J. P., Hoagland, R. G. & Kanninen, M. F. A new representation of the strain field assoceated with the cube-edge dislocation of a-iron. *J. Appl. Phys.* 43, 3921–3933 (1972).
6. Ismail-Beigi, S. & Arias, T. A. *Ab initio* study of screw dislocations in Mo and Ta: a new picture of plasticity in bcc transition metals. *Phys. Rev. Lett.* 84, 1499–1502 (2000).
7. Yang, L. H., Söderlind, P. & Moriarty, J. A. Accurate atomistic simulation of (a/2)<111> screw dislocations and other defects in bcc tantalum. *Phil. Mag. A* 81, 1355–1385 (2001).
8. Kaplan, T., Liu, F., Mostoller, M., Chisholm, M. F. & Milman, V. First-principles study of impurity segregation in edge dislocations in Si. *Phys. Rev. B* 61, 1674–1676 (2000).
9. Liu, F., Mostoller, M., Chisholm, M. F. & Kaplan, T. Electronic and elastic properties of edge dislocations in Si. *Phys. Rev. B* 51, 17192–17195 (1995).
10. Bigger, J. R. K. *et al.* Atomic and electronic structures of the 90° partial dislocation in silicon. *Phys. Rev. Lett.* 69, 2224–2227 (1992).
11. Heggie, M. I., *et al.* Glide dislocations in dimond: first-principles calculations of similarities with and differences from silicon and the effects of hydrogen. *J. Phys. Condens. Matter* 14, 12689–12696 (2002).
12. Martsinovich, N. Heggie, M. I. & Ewels, C. P. First-principles calculations on the structure of hydrogen aggregates in silicon and diamond. *J. Phys. Condens. Matter* 15, S2815–S2824 (2003).
13. Rabier, J., Soullard, J. & Puls, M. P. Atomic calculations of point-defect interactions with an edge dislocation in NiO. *Phil. Mag. A* 61, 99–108 (1990).
14. Rabier, J. & Puls, M. P. On the core structures of edge dislocations in NaCl and MgO. Consequences for the core configurations of dislocation dipoles. *Phil. Mag. A* 59, 821–842 (1989).
15. Puls, M. P., Woo, C. H. & Norgett, M. J. Shell-model calculations of interaction energies between point defects and dislocations in ionic crystals. *Phil. Mag.* 36, 1457–1472 (1977).
16. Puls, M. P. & Norgett, M. J. Atomic calculation of the core structure and Peierls energy of an (a/2)[110] edge dislocation in MgO. *J. Appl. Phys.* 47, 466–477 (1976).
17. Puls, M. P. Vacancy-dislocation interactions energies in MgO A re-analysis. *Phil. Mag. A* 47, 497–513 (1983).
18. Puls, M. P. Vacancy-dislocation interaction energies in MgO. *Phil. Mag. A* 41, 353–368 (1980).
19. Hoagland, R. G., Hirth, J. P. & Gehlen, P. C. Atomic simulation of the dislocation core structure and Peirels stress in alkali halide. *Phil. Mag.* 34, 413–439 (1976).
20. Watson, G. W., Kelsey, E. T. & Parker, S. C. Atomistic simulation of screw dislocations in rock salt structured materials. *Phil. Mag. A* 79, 527–536 (1999).
21. Dumrul, S., Bazzana, S., Warzywoda, J., Biederman, R. R. & Sacco, A. Imaging of crystal growth-induced fine surface features in zeolite A by atomic force microscopy. *Micropor. Mesopor. Mater.* 54, 79–88 (2002).
22. Nabarro, F. R. N. *Theory of Dislocations* (Oxford Univ. Press, Oxford, 1967).
23. Binder, G., Scandella, L., Schumacher, A., Kruse, N. & Prins, R. Microtopographic and molecular scale observations of zeolite surface structures: Atomic force microscopy on natural heulandite. *Zeolites* 16, 2–6 (1996).
24. Agger, J. R., Pervaiz, N., Cheetham, A. K. & Anderson, M. W. Crystallization in zeolite A studied by atomic force microscopy. *J. Am. Chem. Soc.* 120, 10754–10759 (1998).
25. Agger, J. R., Hanif, N. & Anderson, M. W. Fundamental zeolite crystal growth rates from simulation of atomic force micrographs. *Angew. Chem. Int. Edn* 40, 4065–4067 (2001).
26. Faux, D. A., Smith, W. & Forester, T. R. Molecular dynamics studies of hydrated and dehydrated Na+-zeolite-4A. *J. Phys. Chem. B* 101, 1762–1768 (1997).
27. Slater, B., Titiloye, J. O., Higgins, F. M. & Parker, S. C. Atomistic simulation of zeolite surfaces. *Curr. Opin. Solid State Mater. Sci.* 5, 417–424 (2001).
28. Smit, B. & Siepmann, J. I. Simulating the adsorption of alkanes in zeolites. *Science* 264, 1118–1120 (1994).
29. Auerbach, S. M. Theory and simulation of jump dynamics, diffusion and phase equilibrium in nanopores. *Int. Rev. Phys. Chem.* 19, 155–198 (2000).
30. Henson, N. J., Cheetham, A. K. & Gale, J. D. Theoretical Calculations on Silica Frameworks and Their Correlation with Experiment. *Chem. Mater.* 6, 1647–1650 (1994).
31. Poirier, J. P. Rheology of ices: a key to the tectonics of the ice moons of Jupiter and Saturn. *Nature* 299, 683–688 (1982).
32. Nelson, J. Growth mechanisms to explain the primary and secondary habits of snow crystals. *Phil. Mag. A* 81, 2337–2373 (2001).

©2004 Nature Publishing Group

33. Li, L., Raterron, P., Weider, D. & Chen, J. Olivine flow mechanisms at 8 GPa. *Phys. Earth Planet. Inter.* 138, 113–129 (2003).
34. Sanders, M. J., Leslie, M. & Catlow, C. R. A. Interatomic potentials for SiO_2. *JCS Chem. Commun.* 1271–1273 (1984).
35. Wolf, D., Keblinski, P., Phillpot, S. R. & Eggebrecht, J. Exact method for the simulation of Coulombic systems by spherically truncated, pairwise r^{-1} summation. *J. Chem. Phys.* 110, 8254–8282 (1999).
36. Gale, J. D. & Rohl, A. L. The general utility lattice program (GULP). *Mol. Simulat.* 29, 291–341 (2003).
37. Cheetham, A. K., Eddy, M. M., Jefferson, D. A. & Thomas, J. M. A Study of Si,Al ordering in thallium zeolite-a by powder neutron-diffraction. *Nature* 299, 24–26 (1982).
38. Bell, R. G., Jackson, R. A. & Catlow, C. R. A. Lowenstein rule in zeolite-a — a computational study. *Zeolites* 12, 870–871 (1992).
39. Hull, D. & Bacon, D. J. *Introduction to Dislocations* (Pergamon, Oxford, 1984).
40. Steeds, J. W. *Introduction to Anisotropic Elasticity Theory of Dislocations* (Clarendon, Oxford, 1973).
41. Sinclair, J. E., Gehlen, P. C., Hoagland, R. G. & Hirth, J. P. Flexible boundary conditions and nonlinear geometric effects in atomic dislocation modeling. *J. Appl. Phys.* 49, 3890–3897 (1978).
42. Hirth, J. P. Anisotropic elastic solutions for line force arrays. *Scripta Metall.* 6, 535–540 (1972).
43. Rao, S., Hernandez, D., Simmonds, J. P., Parthasarathy, T. A. & Woodward, C. Green's function boundary conditions in two-dimensional and three-dimensional atomistic simulations of dislocations. *Phil. Mag. A* 77, 231–256 (1998).

Acknowledgements

We thank Al Sacco Jr and colleagues for the AFM image shown in Fig. 1. B.S. wishes to acknowledge useful discussions with Jonathan Agger. We thank EPSRC for funding for local computer resources (GR/S06233/01), access to the UK capability computing resource (HPCx) via the Materials Chemistry Consortium (GR/S13422/01) and a studentship to A.M.W. J.D.G. gratefully acknowledges the support of the Government of Western Australia through a Premier's Research Fellowship. K.W. thanks the Royal Society for support under their University Research Fellowship scheme.
Correspondence and requests for materials should be addressed to A.M.W. and B.S.
Supplementary Information accompanies the paper on www.nature.com/naturematerials

Competing financial interests

The authors declare that they have no competing financial interests

©2004 Nature Publishing Group